Plant Physiol. (1995) 107: 53–62

TE7, An Inefficient Symbiotic Mutant of *Medicago truncatula* Gaertn. cv Jemalong

Véronique Bénaben[1], Gérard Duc, Véronique Lefebvre[2], and Thierry Huguet*

Laboratoire de Biologie Moléculaire des Relations Plantes-Microorganismes, Centre National de la Recherche Scientifique, Institut National de la Recherche Agronomique, BP27 Auzeville, 31326 Castanet-Tolosan Cedex, France, (V.B., V.L., T.H.); and Laboratoire de Génétique et d'Amélioration des Plantes, Institut National de la Recherche Agronomique, BV 1540, 21034 Dijon Cedex, France (G.D.)

A mutagenesis program using ethylmethane sulfonate on *Medicago truncatula* Gaertn cv Jemalong, an annual, autogamous and diploid lucerne, permitted the isolation of a mutant (TE7) unable to establish an effective nitrogen-fixing symbiosis, [Nod$^+$Fix$^-$], with *Rhizobium meliloti* wild-type strains. The mutant phenotype is characterized by an altered infection process that leads to the formation of two kinds of inefficient nodules on the same root system. A certain proportion of the nodules are small, round, and uninfected, with infection threads limited to the outer root cortical cells. Others develop to a normal elongated shape and are infected; bacterial release occurs but the bacteria do not differentiate into bacteroids. The ratio of invaded to uninvaded nodules depends on the bacterial strain used. Throughout the infection process, certain events correlated with the plant defense response against pathogens can be observed: (a) the presence of polyphenolic compounds associated with the walls of infected cells and also with some parts of infection threads in the root cortex; (b) appositions on infection thread walls during the early stage of infection and also within the central tissue of infected nodules; and (c) autophagy of the plant cells that contain released bacteria. Genetic data suggest that the phenotype of TE7 is under monogenic and recessive control; this gene has been designated Mt*sym*1.

The *Rhizobium*-legume N-fixing symbiosis is a highly integrated developmental process characterized by multiple signal exchanges between the two partners: the bacterium *Rhizobium* and the legume plant (Dénarié et al., 1992). Inoculation of legumes by specific strains of *Rhizobium* gives rise to deformation and curling of root hairs, and, concomitantly, induces mitosis in the root cortex that leads to the formation of a nodule primordium (Brewin, 1991). These steps depend in part on the synthesis of lipo-oligosaccharides by bacterial nodulation genes in response to flavones secreted by the leguminous root (Dénarié et al., 1992). Bacteria progress toward this primordium by means of the infection thread. The subsequent development of a meristem from the uninfected cells of the primordium gives rise to a nodule. Bacteria are released from the infection threads into newly divided cells of the primordium. The nodules of most temperate legumes are characterized by indeterminate growth and possess an apical meristem (zone I), an invasion zone (zone II) where infection threads grow and bacteria are released and initiate their differentiation into bacteroids, a narrow interzone II-III characterized by the accumulation of starch, a fixation zone (zone III) where bacteroids convert atmospheric N into ammonia, and a senescent zone (zone IV) (Vasse et al., 1990).

Both plant and bacterial mutants defective in symbiotic N fixation provide powerful tools with which to analyze the contribution of both partners to nodule development and function. The availability of numerous bacterial mutants has led to the characterization of many symbiotic steps (for a review of bacterial genes involved in the first steps of nodulation, see Long, 1992). However, by comparison with symbiotic bacterial mutants, relatively few legume mutants defective in symbiotic N fixation have been identified so far (for a review, see Phillips and Teuber, 1992). Until now, the legume plants that have been subjected to mutagenesis programs include pea (Kneen and Larue, 1988; Duc and Messager, 1989), soybean (Carroll et al., 1985), and *Melilotus alba* (Utrup et al., 1993), using either EMS or γ-irradiation. Phenotypes of the plant mutants obtained are commonly grouped into three classes: (a) no nodulation or nodulation that is blocked at a very early stage, [Nod$^-$]; (b) nodules that do not fix N, [Nod$^+$Fix$^-$]; and (c) many more nodules that are produced compared to the wild-type plant, [Nod^{++}Fix$^+$] (Carroll et al., 1985). This last phenotype has not been observed after inoculation with bacterial mutants.

One of the most studied legume-*Rhizobium* interactions is that between alfalfa (*Medicago sativa*) and *Rhizobium meliloti*. Many mutants of *R. meliloti* have been obtained, and purified bacterial nodulation factors are available (Dénarié et al., 1992). Unfortunately, alfalfa is an autotetraploid and allogamous plant with complex genetics and therefore not suited for a mutagenesis program. Furthermore, there are few naturally occurring alfalfa mutants

[1] V.B. is supported by a fellowship from the Ministére de l'Enseignement Supérieur et de la Recherche.

[2] Present address: Station d'Amélioration des Plantes Maraîchères, Institut National de la Recherche Agronomique, Avignon, BP 94, 84143 Montfavet, France.

* Corresponding author; e-mail thuguet@toulouse.inra.fr; fax 33-61-28-50-61.

Abbreviations: DAI, days after inoculation; EMS, ethylmethane sulfonate.

(Peterson and Barnes, 1981). To circumvent this, *Medicago truncatula* Gaertn. has been proposed as a legume model plant for studying symbiosis-related plant genes (Barker et al., 1990). This plant, efficiently nodulated by *R. meliloti*, is annual, diploid, and autogamous. Its genome is 4-fold smaller than that of *M. sativa* and a number of symbiotic genes have already been characterized and sequenced (Gallusci et al., 1991; Pichon et al., 1992; Stanford et al., 1993).

A mutagenesis program using EMS has been carried out with *M. truncatula* cv Jemalong and has led to the isolation of a [Nod^+Fix^-] mutant. We provide evidence that plant defense reactions are elicited throughout nodulation of this mutant and are associated with the infection process. Modified infection results in the formation of two kinds of nodules on the same root system after inoculation with *R. meliloti*. Certain of these are small and devoid of bacteria, whereas others are elongated and infected. In the latter case, bacteria are released but these are unable to differentiate into bacteroids.

MATERIALS AND METHODS

Plant Material and Bacterial Strains

Medicago truncatula cv Jemalong was provided by P. Guy (Plant Breeding Station, Institut National de la Recherche Agronomique, Lusignan, France). A subpopulation of *M. truncatula* cv Jemalong, called 2828, was selected (G. Genier, unpublished results) and used for all the experiments. A homozygous genotype (J5) derived from a single seed of the 2828 subpopulation was used for the crosses with the mutant TE7. The following strains of *Rhizobium meliloti* that form effective nodules on *M. truncatula* cv Jemalong were tested with the TE7 mutant: 2011, 102F51, S33 (Casse et al., 1979), CC169 (Brockwell and Hely, 1966), and ABS7 (Bekki et al., 1987). To localize bacteria during structural studies, we used the strains 2011 and ABS7 into which the plasmid XLGD4 had been introduced (M. Ghérardi, unpublished results). This plasmid carries the constitutively expressed *hem*A::*lac*Z fusion (Leong et al., 1985).

EMS Mutagenesis

One thousand five hundred seeds of *M. truncatula* cv Jemalong subpopulation 2828 were scarified with abrasive paper and then soaked for 24 h without aeration at 24°C in 45 mL of an aqueous solution containing 0.2% of EMS. Treated seeds were washed under running water for 1 h before being sown in a greenhouse (temperature 15–22°C with additional lighting to assure a 16-h photoperiod). Due to the autogamous character of this species (Crawford et al., 1989), no special protection from foreign pollination was used for successive progeny production. The 400 M_1 plants that successfully germinated produced, after spontaneous selfing, approximately 250,000 M_2 seeds, which were harvested as a single batch. Only 17,000 M_2 plants were grown in the greenhouse, using sand with a granular size of less than 3 mm, and inoculated with *R. meliloti* strain 2011 at the time of sowing. Plants were watered daily with a N-free nutrient solution (Duc and Messager, 1989) and screened 40 to 50 d after sowing by uprooting and washing the root system. Plants with chlorotic shoots were screened for either the complete absence of nodules or the presence of nonfixing white nodules (deficient in leghemoglobin) and replanted in the same substrate and watered with a nutrient solution containing 15 mM combined N (Duc and Messager, 1989). M_3 and M_4 progenies from these putative mutants (30 plants per progeny) were retested using the same screening procedure as for the M_2 generation to study the heritability and genetic stability of the M_2 phenotype.

One mutant, TE7, was crossed with the J5 genotype of *M. truncatula*; cross-pollination was carried out at the bud stage of flower development after emasculation under the binocular microscope. A cellophane bag was placed over pollinated flowers to maintain humidity.

Plant Growth Conditions for Structural Studies

After surface-sterilization of seeds (Barker et al., 1990), two different growth conditions were used. Plants were grown on N-free agar slants in test tubes (Farhåeus, 1957) and, after inoculation with a culture of *R. meliloti*, were used to study nodulation kinetics. Alternatively, axenic seedlings were grown aeroponically (Gallusci et al., 1991) with a nutrient medium containing N. Two weeks later, the solution was replaced with a N-free nutrient solution and the plants were inoculated 48 h later. Several days after infection, nodule samples were harvested for structural and ultrastructural studies.

Histological Studies

Nodules were fixed in 2.5% glutaraldehyde in 0.2 M sodium cacodylate, pH 7.2, for 30 min under vacuum and for 1 h at atmospheric pressure, then washed with 0.2 M sodium cacodylate, pH 7.2, and histochemically stained for β-galactosidase activity as described by Boivin et al. (1990). Roots and nodules were observed either as intact organs or after thick sectioning (80 μm) with a Bio-Rad microcut H1200.

For thin and semi-thin sections, nodules were fixed in 2.5% glutaraldehyde for 1 h under vacuum and for 2 h at atmospheric pressure, and then washed with 0.2 M sodium cacodylate, pH 7.2, and postfixed in 2% osmium tetroxide, dehydrated in an alcohol series, and embedded in Epon (Vasse et al., 1993). Semi-thin sections were stained with basic 2% fuchsin and with a mixture of 0.2% methylene blue, 1% toluidine blue in 1% sodium borate aqueous solution (Millonig, 1976). Ultra-thin sections for EM were stained with uranyl acetate and lead citrate (Reynolds, 1963) and observed with an Hitachi EM600 electron microscope.

Staining for Polyphenols

Infected roots of whole plants were treated with a solution of potassium permanganate to visualize polyphenols as described by Vasse et al. (1993). For semi-thin sections, nodules and infected roots were fixed as above, dehydrated in an alcohol series, and embedded in LR White

acrylic resin at 65°C. Autofluorescence due to polyphenols was observed under UV illumination before staining with 0.02% toluidine blue in distilled water (Vasse et al., 1993). Toluidine blue leads to metachromatic reactions: blue staining for polyphenolics, violet staining for other wall compounds (Kovats et al., 1991). Observations and photography for light microscopy were made with an Olympus Vanox light microscope (Tokyo, Japan).

Statistical Analysis

The analysis of the percentages of invaded and uninvaded nodules was performed with 20 plants grown in test tubes, 24 DAI with the *R. meliloti* strains 2011, ABS7, and CC169. The experiment was repeated twice. The roots were cleared with a commercial solution of sodium hypochlorite according to Truchet et al. (1989), rinsed with distilled water, stained with methylene blue (0.01%), and observed microscopically. We used logistic transformation to analyze the ratio of invaded nodules to uninvaded nodules using the method of Cox and Snell (1991), and the resulting data were analyzed by Dunnett's *t* test.

RESULTS

Isolation of a [Nod$^+$Fix$^-$] Monogenic Mutant

After screening 17,000 M_2 plants, we identified a [Nod$^+$Fix$^-$] mutant (named TE7) whose phenotype was stable in the M_3 and M_4 generations and that was not affected in its fertility. Progenies of TE7 have been observed over three generations (M_3 to M_5), with no noticeable modification to the phenotype. No morphological or nonsymbiotic developmental differences could be observed between TE7 and *M. truncatula* 2828 subpopulation plants (data not shown). Also, there was no difference in root growth between TE7 and the wild type, either with or without inoculation. However, TE7 plants could not grow without exogenous N and no N fixation could be detected (absence of acetylene reduction, data not shown) after inoculation with any of the five wild-type strains of *R. meliloti* tested (see "Materials and Methods"). All five strains elicited phenotypically identical, ineffective nodules on TE7.

Detailed analysis of nodulation were carried out with the strains 2011, CC169, and ABS7. The number of nodules per plant mutant was slightly higher than that observed for wild-type plants (Table I). However, the kinetics of nodulation are similar: the first bumps appeared at 5 DAI and all plants were nodulated at 12 DAI (data not shown). All the structural studies described below were carried out on nodules elicited by *R. meliloti* 2011 (pXLGD4).

Table I. *Average number of nodules (±SD) per plant for wild type and TE7 M. truncatula inoculated with the strains 2011, ABS7, and CC169 of R. meliloti*

For each condition, 15 plants were grown in test tubes and nodule numbers were counted 24 DAI. Identical letters means that the nodule averages per plant are not significantly different at P = 5% using Student's *t* test.

	2011	ABS7	CC169
Wild type	10.7 ± 3.2 a	7.6 ± 2.8 b	5.1 ± 1.4 c
TE7	12.5 ± 2.9 a	10.2 ± 4.1 a,b	7.7 ± 1.8 b

A Defense Response Was Induced Early during the Infection Process

Four to five DAI with *R. meliloti* 2011 (pXLGD4), root hair deformation and infection thread formation (Fig. 1A) could be detected for both wild-type and mutant TE7 plants grown in test tubes. Nodule primordia were elicited at the same time as for the wild-type plant. However, although wild-type nodule primordia were rapidly invaded, infection thread penetration of the nodule primordium of the mutant appeared retarded.

Moreover, during the infection process, pigmented cells were observed in the infected root inner cortex of TE7 plants (Fig. 1A). These cells were stained with potassium permanganate and are adjacent to or traversed by infection threads. Serial semi-thin sections of the TE7-infected root cortex, before invasion of the nodular primordium by infection threads, frequently revealed cells with star-shaped configurations. Such cells were traversed by thick infection threads and contained bacteria in their cytoplasm (Fig. 1, B and C). Their walls and certain regions of the infection threads showed a metachromatic reaction after toluidine blue staining and were autofluorescent, suggesting chemical changes to the wall structure. A similar type of reaction could sometimes be observed during infection of wild-type plants, but in such cases this occurred in the same location but later, after the invasion of the wild-type primordium by infection threads (data not shown).

After inoculation of the TE7 mutant, two kinds of white nodules could be observed on the root system of all plants tested, whereas only pink nodules were found on wild-type plants. The first type comprised small hemispherical nodules frequently covered by a mass of yellow cells; the second type were elongated. Both the small round and the elongated nodules were observed, with no apparent specific spatio-temporal distribution, on the entire root system (data not shown).

Small, Round Nodules Are Not Infected

Small nodules measured about 1 mm in diameter and were characterized by partially developed peripheral vascular bundles surrounding a central tissue devoid of bacteria (Fig. 1D). At the distal end of the central tissue, small cells with a dense cytoplasm appeared meristematic in character, but cell divisions were not observed (data not shown).

Bacteria localized in infection threads were found only in a mass of cells located on the top of the nodule. This collection of cells appears to be the remains of the external root cortex. A similar structure could also be observed in young developing wild-type nodules (8–10 DAI) but was peeled off early in nodule development (data not shown).

As observed during the infection process, only the walls of cells that were traversed by infection threads showed a metachromatic reaction with toluidine blue and were

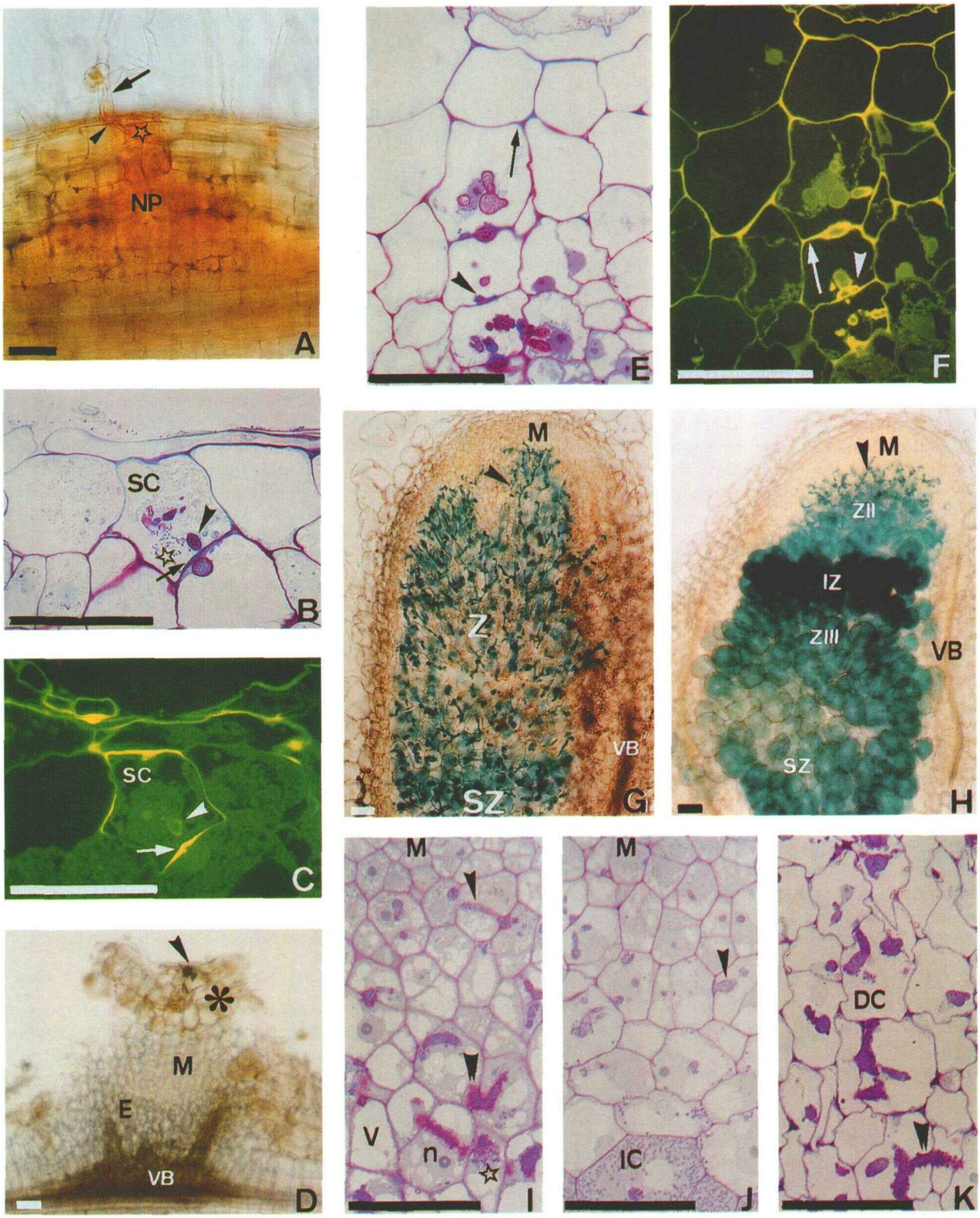

Figure 1. Infection of TE7 by *R. meliloti* 2011 (pXLGD4). Bars equal 70 μm throughout. A, Root of *M. truncatula* TE7 mutant 6 DAI. Pigmented cells (star) are stained with permanganate and are in contact with infection threads (arrowhead). Above the nodule primordium (NP), an infection thread is visible in the root hair (arrow). B and C, Semi-thin section (1 μm) of infected root cortex of *M. truncatula* TE7 (6 DAI). B, Stained with toluidine blue. C, Serial semi-thin section of B observed by autofluorescence. Star-shaped cell (SC) is infected; its walls (arrows) are blue and autofluorescent. This cell contains a number of free bacteria (star on B). Parts of the infection thread (arrowhead) are blue and slightly auto-

(Continued on facing page)

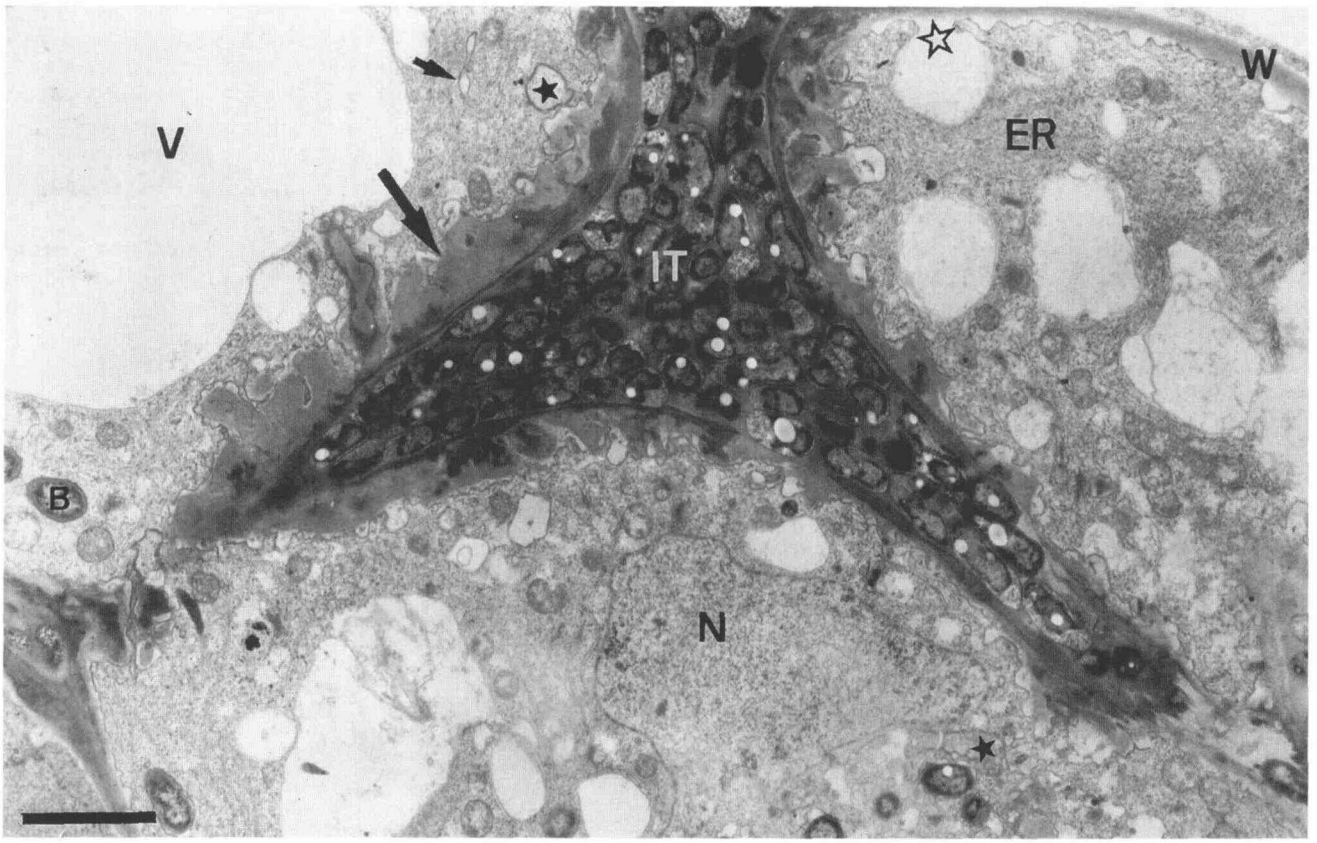

Figure 2. Electron micrograph of cells from a TE7 large nodule. The intercellular infection thread (IT) has thick irregular appositions (large arrow) and bacteria in the infection thread accumulate polyhydroxybutarate (white spots in the bacteria). In the cell to the right, there is a well-developed ER invaginated plasma membrane (open star). In the cell to the left, autophagic vesicles (black star), dilated ER (small arrow), and released bacteria (B) are indicated. Nucleus (N), cell wall (W), and vacuoles (V) are marked. Bar equals 2 μm.

strongly autofluorescent (Fig. 1, E and F). Some regions of the wall of the infection threads were also autofluorescent and stained blue with the toluidine blue reagent. Certain regions of the infection threads appeared thickened.

The Large, Elongated Nodules Are Invaded, but Bacteria Fail to Differentiate

A comparison between thick sections through nodules from TE7 and wild-type plants harvested 21 DAI (Fig. 1, G and H) showed that the large TE7 nodules shared the following characteristics with normal nodules: peripheral vascular bundles, an apical meristem, a peripheral endodermis, and a well-developed central tissue. However, whereas the central tissue of wild-type nodules contained enlarged cells, cells of the mutant nodule central tissue remained small. Also, the characteristic zonation (Vasse et al., 1990) of indeterminate and effective nodules was not visible in large TE7 nodules. It appeared that bacteria were confined to a network of infection threads

Figure 1. *(continued from facing page)* fluorescent. D, Thick section (80 μm) of small nodule (10 DAI) of TE7 mutant after histochemical staining for β-galactosidase activity. Meristem (M), vascular bundles (VB), and endodermis (E) are indicated. Bacteria are localized in infection threads (arrowhead) in the remnants of the nodule cortex (asterisk). E and F, Serial semi-thin sections of the top of small nodule (10 DAI). Parts of the wall of the cell (arrows) traversed by infection threads and intercellular infection threads (arrowheads) stained blue with toluidine blue (E) and are autofluorescent (F). G and H, Thick sections of elongated nodules (15 DAI) from TE7 (G) and wild-type *M. truncatula* (H) after β-galactosidase histochemical staining. The wild-type nodule is divided into meristem (M), invasion zone (ZII), interzone II-III (IZ), fixation zone (ZIII), and senescent zone (SZ), whereas the central tissue of the TE7 nodule is invaded by a network of infection threads (arrowheads) and can be divided into meristem (M), invasion-like zone (Z), and a senescent zone (SZ). Vascular bundles in the peripheral endodermis are visible (VB). I, J, and K, Semi-thin sections of meristem and invasion zone (I) and senescent zone (K) of a large nodule from TE7 and meristem, and invasion zone of a wild-type nodule (J). In the TE7 nodule (I), infection threads with a regular wall (single arrowhead) are observed only close to the meristem (M), whereas the remainder have thick walls (double arrowhead). In the TE7 invasion zone, there are few released bacteria (next to the open star); the vacuole (V) and nucleus (n) are indicated. In the invasion zone of the wild-type nodule (J), infection threads (arrowheads) are found in the distal part just below the meristem (M) and infected cells (IC) in the proximal part. In the senescent zone (K), cells are deformed (DC) and traversed by thick infection threads (double arrowhead).

that were present throughout the central tissue. Nevertheless, semi-thin sections of large TE7 nodules showed that the central tissue was not homogenous and could be divided into three zones, characterized by a progressive vacuolization from the distal to the proximal end. The three zones were: (a) an active apical meristem similar to the wild-type nodule meristem (Fig. 1, I and J); (b) a zone similar to the wild-type invasion zone II where infection threads and bacterial release were visible; and (c) a senescent zone where cells appeared without cytoplasm on semi-thin sections. These cells were often deformed and traversed by infection threads (Fig. 1K).

Occasionally, remnants of the external root cortex could also be observed on the lateral side of these nodules. These cells were traversed by thick infection threads and had the same characteristics as those of small nodules in terms of staining with toluidine blue and autofluorescence (data not shown).

Throughout the central tissue, no metachromatic reactions or strong autofluorescence of walls was observed (data not shown). However, infection threads had thick, irregular walls, with the exception of those close to the meristematic zone. EM revealed that the thickness of the walls was due to fibrillar appositions localized on the outside of the thread wall (Fig. 2). The cellular plasma membrane followed the irregularity of the appositions, creating numerous folds. Inside the infection thread, bacteria were embedded in the gum matrix and accumulated polyhydroxybutyrate.

Bacterial release occurred in the central tissue of large TE7 nodules (Fig. 3, A and B) and such bacteria were surrounded by a peribacteroid membrane. However, they showed few signs of differentiation; there was limited multiplication and the bacteria did not elongate to form bacteroids. The plant cytoplasm in the vicinity of released bacteria (Fig. 3A) was characterized by a large quantity of membrane that was not observed in the wild-type nodule. Some regions of the cytoplasm were sequestered by vesicles with a double membrane, apparently originating from the ER. Mitochondria were occasionally of abnormal shape with dense stroma and inner membranes (Fig. 3B).

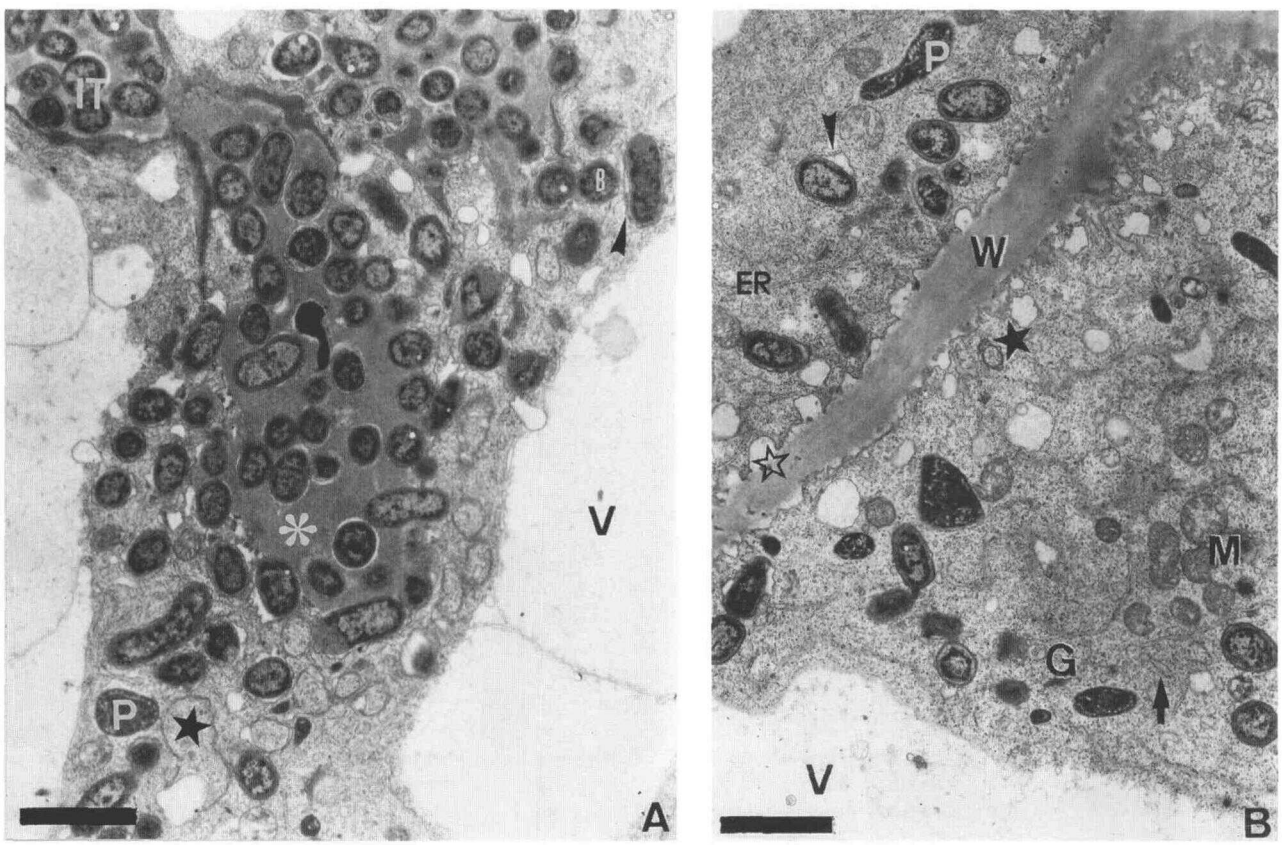

Figure 3. Electron micrograph of the region with released bacteria from elongated nodules of TE7. A, The bacteria (B) are released from an *infection thread* (IT) without appositions, containing gum-matrix (asterisk). Next to the released bacteria, some autophagic vesicles can be seen (black star). The peribacteroid membrane of the released bacteria (arrowhead; also for 3B) is not in contact with the bacteria. B, The cytoplasm of cells in this area contains several organelles such as the ER (ER) and Golgi apparatus (G). However, some of these are modified: certain regions of the ER are dilated (arrow), the *mitochondria* (M) have a dense inner membrane, some autophagic vesicles (next to black star) are present, and there are numerous folds of the plasma membrane (empty star) around the cell wall (W). Proplastids (P) and vacuoles (V) are present in both A and B. Bars equal 2 μm.

Ultrastructural studies of the senescent zone showed a condensation of the plant cell cytoplasm around the infection thread (Fig. 4). Except for the nucleus, all the plant cell organelles were no longer visible, whereas released bacteria were still present in the cytoplasm. In the most proximal region, cells contained only fragments of membranes and bacteria were released passively from damaged infection threads (Fig. 5).

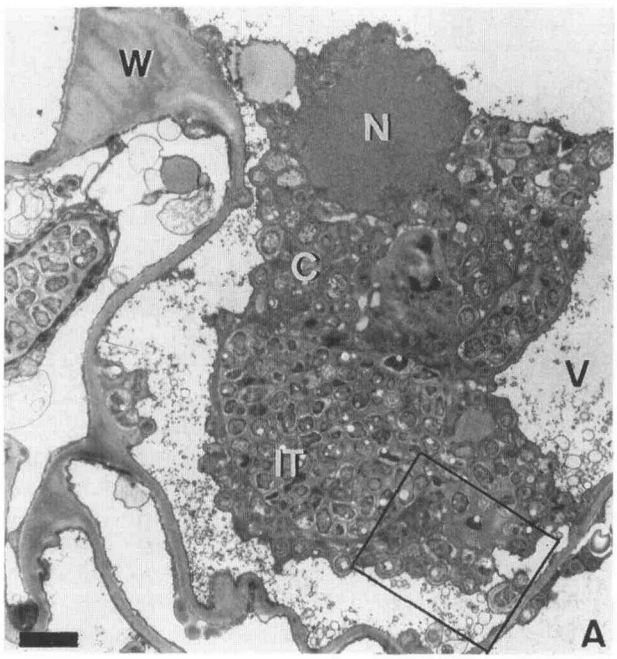

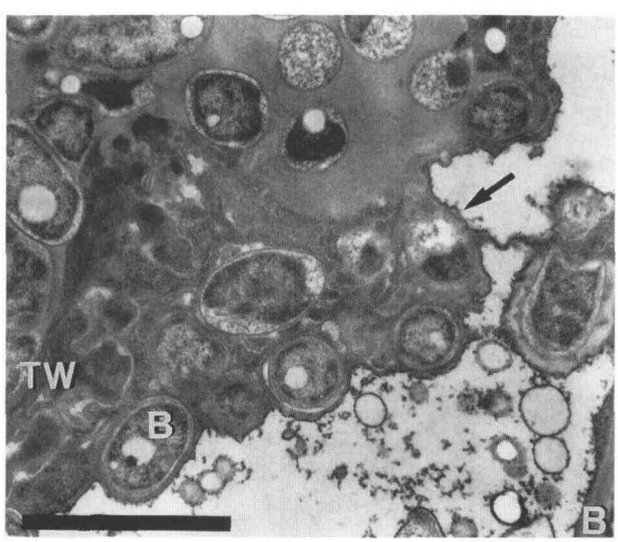

Figure 4. Electron micrograph of cells in the distal part of the senescent zone. A, Cells in the distal part of this zone have a large vacuole (V), condensed cytoplasm (C), nucleus (N), and infection thread (IT). Cells have deformed walls (W). B, Enlarged detail of A, showing released bacteria (B) in the condensed cytoplasm limited by the tonoplast (arrow). There are appositions (TW) on the infection thread. Bars equal 2 μm.

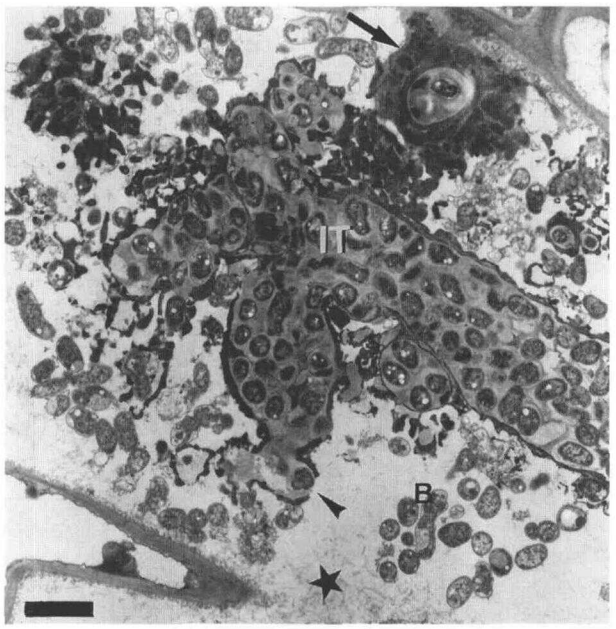

Figure 5. Senescence in the most proximal cells of the nodule. The cytoplasm has completely degenerated, containing only membrane ghosts (star), infection threads (IT), and bacteria (B). Some regions of the infection threads have very thick walls (arrow), whereas others are crushed. Bacteria are released passively (arrowhead) and subsequently degenerate. Bar equals 2 μm.

The Invasion of the Primordium Is Bacterial Strain Dependent

The percentage of invaded and uninvaded nodules 24 DAI varies according to the *R. meliloti* strain used for inoculation (Fig. 6). Fifty-five percent of nodules induced by ABS7 and 70% induced by CC169 were invaded by infection threads, compared with only 30% of nodules induced by *R. meliloti* 2011. The differences between the strain 2011 and the strains ABS7 or CC169 are statistically significant for P = 5%. Cytological observations of elongated nodules induced by the strain ABS7 showed the same cytological features as those elicited by the strain 2011: polyphenol depositions and appositions on walls of infection threads. No additional bacteria in the host cell cytoplasm could be observed (data not shown).

The TE7 Mutation Appears to Be Monogenic and Recessive

To genetically characterize the mutant TE7, we studied a cross between TE7 and the genotype J5 (see "Materials and Methods"). As shown in Table II, a segregation of 161[Fix^+]/41[Fix^-] was obtained in the F_2. This segregation pattern is statistically consistent with a Mendelian inheritance pattern in which the Fix^- phenotype is determined by a single recessive allele.

DISCUSSION

EMS mutagenesis of the legume model plant *M. truncatula* cv Jemalong has led to the isolation of the TE7 symbiotic mutant, a stable [Nod^+Fix^-] mutant line. Unlike sev-

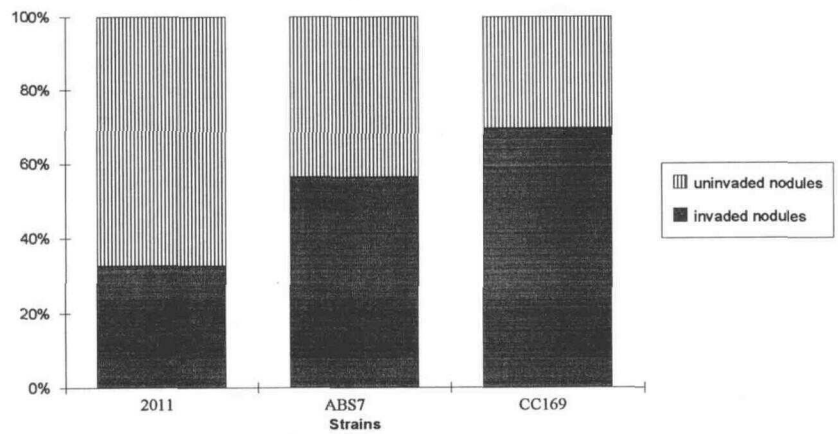

Figure 6. Percentages of the two kinds of nodules, invaded and uninvaded, on the entire root system 24 DAI. For each condition more than 30 plants were grown, representing at least 250 nodules for each.

eral symbiotic plant mutants such as the pea *sym17* mutant (Lee and LaRue, 1992) or certain soybean hypernodulating mutants (Carroll et al., 1985), no gross morphological alterations were apparent for TE7 plants. This mutation does not alter the nodulation potential and neither the number nor the kinetics of nodulation was significantly altered. Furthermore, the phenotype could not be overcome by any of the *R. meliloti* strains tested, as is the case for certain mutants of pea, soybean, or *Vicia faba*, for which the phenotype has been shown to be strain dependent (Phillips and Teuber, 1992).

The TE7 mutant phenotype is characterized by the formation of two classes of inefficient nodules that can be correlated with the extent of invasion of the primordium by the infection threads. The first class is characterized by elongated nodules whose central tissue is filled with a large network of infection threads with thick walls. These nodules do not show the characteristic zonation of wild-type indeterminate nodules; they possess a meristem and a large invasion zone (zone II-like) where bacterial release takes place, but there is little if any bacterial development [Bad^-] (Vincent, 1980). Finally, in the proximal part of the nodule, a large zone of senescence is visible and there is evidence for plant cell senescence as soon as bacteria are released. This evidence includes both sequestration of the cytoplasm by the ER and vacuolization, classical signs of cell degeneration and autophagy (Dunn, 1990). Early senescence has often been described in the situation where bacteria are released within nodules but cannot differentiate into bacteroids. Such nodules result from the interaction of either bacterial mutant and wild-type plant (T8–1 *Bradyrhizobium japonicum* mutant and soybean [Morrison and Verma, 1987]; *R. meliloti ndv* mutant and alfalfa [Quandt et al., 1992]; neomycin-resistant mutant of *R. meliloti* and alfalfa [Reddy et al., 1992]) or plant mutant and wild-type bacteria (*in1* mutant of alfalfa [Vance and Johnson, 1983]; *sym* 1 mutant of *Vicia faba* [Häser et al., 1992]).

A second class of nodule can also be found on roots of the mutant TE7, a situation that has already been described for certain mutants of *R. meliloti* (Putnoky et al., 1988). In the case of TE7, this second category comprises nodules devoid of bacteria, similar to those induced on the *sym2* mutant of pea (Le Gal and Hobbs, 1989), or elicited on alfalfa after inoculation with *R. meliloti exo* mutants (Yang et al., 1992), or elicited on bean with certain lipopolysaccharide-defective mutants of *R. phaseoli* (Noel et al., 1986).

For the TE7 mutant, the ratio of empty to invaded nodules depends on the strain of *R. meliloti*. Wild-type strains such as ABS7 and CC169 appear to be more efficient at invading nodule primordia compared with the laboratory strain 2011. Although the biochemical and genetic basis of this difference is not known, this suggests that the existence of two classes of nodules is only an indirect consequence of the plant mutation and may result from the activation of a defense mechanism. It could be of interest to investigate whether the extent of infection thread progression is correlated with nodulation efficiency on a wild-type plant.

The presence of two classes of nodules on the TE7 plant reveals an interesting correlation between bacterial invasion and nodule meristem activity. Abortion of infection

Table II. *Segregation of the [Nod^+Fix^-] phenotype in the F_1 and F_2 generations resulting from the crossing TE7♀ × J5♂*

The calculated χ^2 values indicate that the segregation is consistent with Mendelian inheritance as a monogenic and recessive mutation with 1 *df*, at the P 15% significance level. Tabulated χ^2 is 3.84 at P = 5%.

Generation	Genotype	No. of Plants		χ^2 of 3/1 [Nod^+Fix^+]/[Nod^+Fix^-]
		[Nod^+Fix^+]	[Nod^+Fix^-]	
Parental lines	J5	30	0	
	TE7	0	30	
F_1	TE7♀ × J5♂	1	0	
F_2		161	41	2.38

threads in the root cortex is correlated with the formation of small nodules, whereas invasion of the primordium leads to elongated nodules with an active meristem. This is consistent with previous findings that nodule organogenesis can be induced by the invading bacteria at a distance, most probably due to the effect of bacterial lipo-oligosaccharide Nod factors (Dénarié et al., 1992). However, the persistence of meristematic activity appears to require the invasion of the primordium by infection threads. This supports the hypothesis that the continuous growth of the nodule meristem depends on the production of unknown growth-stimulating substances by the invading bacteria (Truchet et al., 1980; Yang et al., 1992).

During the entire infection process, the progression of the infection threads is accompanied by plant reactions that resemble those previously described in plant-pathogen interactions and that are interpreted as plant defense responses (Agrios, 1988; Kovats et al., 1991). First, an accumulation of polyphenolic compounds can be observed in the infected root cortex, similar to that observed during the inefficient interaction between a normal plant and a symbiotic bacterial mutant such as that between *R. meliloti exo* mutants and alfalfa (Niehaus et al., 1993) or between *R. leguminosarum lps* mutants and pea (Perotto et al., 1994). This kind of defense response can also be observed at sites of aborted infection when alfalfa is inoculated with its regular symbiont (Vasse et al., 1993). It is interesting to note that, in contrast to nodules induced by *lps* mutants of *R. leguminosarum* (Perotto et al., 1994), polyphenols are limited to the plant cell walls of root cortical cells for the TE7 mutant and are never observed in the central tissue of the nodules.

Second, the deposition of new wall material on infection threads is observed throughout the nodulation process for the TE7 plant, as is also the case for certain empty nodules (Noel et al., 1986) and certain elongated alfalfa nodules elicited by bacterial mutants (*R. meliloti leu*$^-$ strains [Truchet et al., 1980]; *R. meliloti hemA* mutants [Dickstein et al., 1991]). However, in contrast to TE7 elongated nodules, these nodules do not contain released bacteria. Only the *lps* mutant of *R. leguminosarum* can induce Bad$^-$ nodules with wall deposition on infection threads, but in this case the network of infection threads in the central tissue is not as well developed as in TE7 elongated nodules (Perotto et al., 1994). These data suggest that invaded nodules of the TE7 mutant represent a novel phenotype.

Genetic analysis of the TE7 mutant provides strong evidence that the mutation is monogenic and recessive, and we propose to name the mutated gene Mt*sym*1. For most symbiotic plant mutants, the mutation has also been determined to be monogenic and recessive (Duc and Messager, 1989; Weeden et al., 1990). However, in the case of the TE7 mutant, we cannot exclude the possibility that two closely associated loci could have been altered during the mutagenesis treatment, as has been shown for the NN5 mutant of soybean (Pracht et al., 1993) and for the *sym13* mutant of pea (Kneen et al., 1990).

In conclusion, the Fix$^-$ phenotype of the TE7 mutant is strongly correlated with the block of bacteroid differentiation and also with defense reactions that are present throughout the infection process and visible as early as the appearance of the first invaded cells of the root cortex. Although it is possible to explain the presence of the two classes of nodules by a bacterial strain-dependent slowing down of infection thread progression, it remains unclear if the defense reactions are the cause or the consequence of the Fix$^-$ phenotype. Therefore, TE7 could be a useful tool for studying the relationship between defense and symbiotic processes during rhizobial infection.

ACKNOWLEDGMENTS

We thank H. De Larambergue, F. Moussy, and R. Bodergat for their technical assistance in the mutagenesis program, A. Moisan for her help in statistical analysis, F. de Billy, R. Dickstein, and J. Vasse for their interest and comments, and D. Barker and C. Grosjean for their critical reading and assistance in the preparation of the manuscript.

Received June 6, 1994; accepted September 29, 1994.

LITERATURE CITED

Agrios GN (1988) How plants defend themselves against pathogens. *In* BJ Harcourt, ed, Plant Pathology. Academic Press, San Diego, CA, pp 97–115

Barker DG, Bianchi S, Blondon F, Dattée Y, Duc G, Flament P, Gallusci P, Génier P, Guy P, Muel X, Tourneur J, Dénarié J, Huguet T (1990) *Medicago truncatula*, a model plant for studying the molecular genetics of the *Rhizobium*-legume symbiosis. Plant Mol Biol Rep **8:** 40–49

Bekki A, Trinchant J-C, Rigaud J (1987) Nitrogen fixation (C_2H_2 reduction) by *Medicago* nodules and bacteroids under sodium chloride stress. Physiol Plant **71:** 61–67

Boivin C, Camut S, Malpica CA, Truchet G, Rosenberg C (1990) *Rhizobium meliloti* genes encoding catabolism of trigonelline are induced under symbiotic conditions. Plant Cell **2:** 1157–1170

Brewin NJ (1991) Development of the legume root nodule. Annu Rev Cell Biol **7:** 191–226

Brockwell J, Hely FW (1966) Symbiotic characteristics of *Rhizobium meliloti*: an appraisal of the treatment of nodulation and nitrogen fixation interactions between hosts and rhizobia of diverse origins. Aust J Agric Res **17:** 885–899

Carroll BJ, McNeil DL, Gresshoff PM (1985) Isolation and properties of soybean [*Glycine max* (L.) Merr.] mutants that nodulate in the presence of high nitrate concentrations. Proc Natl Acad Sci USA **82:** 4162–4166

Casse F, Boucher C, Julliot JS, Michel M, Dénarié J (1979) Identification and characterization of large plasmids in *Rhizobium meliloti* using agarose gel electrophoresis. J Gen Microbiol **113:** 229–242

Cox DR, Snell EJ (1991) Analysis of Binary Data. Chapman and Hall, New York

Crawford EJ, Lake AWH, Boyce KG (1989). Breeding annual *Medicago* species for semiarid conditions in Southern Australia. Adv Agron **42:** 399–437

Dénarié J, Debellé F, Rosenberg C (1992) Signaling and host range variation in nodulation. Annu Rev Microbiol **46:** 497–531

Dickstein R, Scheirer DC, Fowle WH (1991) Nodules elicited by *Rhizobium meliloti* heme mutants are arrested at an early stage of development. Mol Gen Genet **230:** 423–432

Duc G, Messager A (1989) Mutagenesis of pea (*Pisum sativum* L.) and the isolation of mutants for nodulation and nitrogen fixation. Plant Sci **60:** 207–213

Dunn WA (1990) Studies on the mechanisms of autophagy: formation of the autophagic vacuole. J Cell Biol **110:** 1923–1933

Farhåeus G (1957) The infection of white clover root hairs by nodule bacteria studied by a simple slide technique. J Gen Microbiol **16:** 374–381

Gallusci P, Dedieu A, Journet EP, Huguet T, Barker DG (1991) Synchronous expression of leghemoglobin genes in *Medicago truncatula* during nitrogen-fixing root nodule development and response to exogenously supplied nitrate. Plant Mol Biol **17:** 335–349

Häser A, Robinson DL, Duc G, Vance CP (1992) A mutation in *Vicia faba* results in ineffective nodules with impaired bacteroid differentiation and reduced synthesis of late nodulins. J Exp Bot **43:** 1397–1407

Kneen BE, LaRue TA (1988) Induced symbiosis mutants of pea (*Pisum sativum*) and sweetclover (*Melilotus alba*). Plant Sci **58:** 177–182

Kneen BE, LaRue TA, Hirsch AM, Smith CA, Weeden NF (1990) *sym* 13, a gene conditioning ineffective nodulation in *Pisum sativum*. Plant Physiol **94:** 899–905

Kovats K, Binder A, Hohl HR (1991) Cytology of induced systemic resistance of cucumber to *Colletotrichum lageranium*. Planta **183:** 484–490

Lee HK, LaRue TA (1992) Pleiotropic effects of *sym*-17. A mutation in *Pisum sativum* L. cv Sparkle causes decreased nodulation, altered root and shoot growth, and increased ethylene production. Plant Physiol **100:** 1334–1338

Le Gal MF, Hobbs LA (1989) Cytological studies of the infection process in nodulating and nonnodulating pea genotypes. Can J Bot **67:** 2435–2443

Leong S, Williams P, Ditta G (1985) Analysis of the 5′ regulatory region of the gene for δ-aminolevulinic acid of *Rhizobium meliloti*. Nucleic Acids Res **13:** 5967–5978

Long SL (1992) Genetic analysis of *Rhizobium* nodulation. *In* G Stacey, RH Burris, HJ Evans, eds, Biological Nitrogen Fixation. Chapman and Hall, New York, pp 561–595

Millonig G (1976) Laboratory Manual of Biological Electron Microscopy. M Savido, Vercelli, Italy

Morrisson N, Verma DPS (1987) A block in the endocytosis of *Rhizobium* allows cellular differentiation in nodules but affects the expression of some peribacteroid membrane nodulins. Plant Mol Biol **9:** 185–196

Niehaus K, Kapp D, Pühler A (1993) Plant defense and delayed infection of alfalfa pseudonodules induced by an exopolysaccharide (EPS-I)-deficient *Rhizobium meliloti* mutant. Planta **190:** 415–425

Noel KD, VandenBosch KA, Kulpaca B (1986) Mutation in *Rhizobium phaseoli* that leads to arrested development of infection threads. J Bacteriol **168:** 1392–1401

Perotto S, Brewin NJ, Kannenberg EL (1994) Cytological evidence for a host defense response that reduces cell and tissue invasion in pea nodules by lipopolysaccharide-defective mutants of *Rhizobium leguminosarum* strain 3841. Mol Plant Microbe Interact **7:** 99–112

Peterson MA, Barnes DK (1981) Inheritance of ineffective nodulation and non-nodulation traits in alfalfa. Crop Sci **21:** 611–616

Phillips DA, Teuber LR (1992) Plant genetics of symbiotic nitrogen fixation. *In* G Stacey, R Burris, HJ Evans, eds, Biological Nitrogen Fixation. Chapman and Hall, New York, pp 625–647

Pichon M, Journet EP, Dedieu A, De Billy F, Truchet G, Barker DG (1992) *Rhizobium meliloti* elicits transient expression of the early nodulin gene ENOD12 in the differentiating root epidermis of transgenic alfalfa. Plant Cell **4:** 1199–1211

Pracht JE, Nickell CD, Harper JE (1993) Genes controlling nodulation in soybean: *Rj*5 and *Rj*6. Crop Sci **33:** 711–713

Putnoky P, Grosskopf E, Cam Ha DT, Kiss GB, Kondorosi A(1988) *Rhizobium fix* genes mediates at least two communication steps in symbiotic nodule development. J Cell Biol **106:** 597–607

Quandt J, Hilleman A, Niehaus K, Arnold W, Pühler A (1992) An osmorevertant of a *Rhizobium meliloti ndv*B deletion mutant forms infection threads but is defective in bacteroid development. Mol Plant Microbe Interact **5:** 420–427

Reddy A, Bochenek B, Hirsch AM (1992) A new *Rhizobium meliloti* symbiotic mutant isolated after introducing *Frankia* DNA sequence into a *nod*A::Tn5 strain. Mol Plant Microbe Interact **5:** 62–71

Reynolds ES (1963) The use of lead citrate at high pH as an electron opaque stain in EM. J Cell Biol **17:** 208–213

Stanford AC, Larsen K, Barker DG, Cullimore JV (1993) Differential expression within the Gln synthetase gene family of the model legume *Medicago truncatula*. Plant Physiol **103:** 73–81

Truchet G, Camut S, de Billy F, Odorico R, Vasse J (1989) The *Rhizobium*-legume symbiosis. Two methods to discriminate between nodules and other derived structures. Protoplasma **149:** 82–88

Truchet G, Michel M, Dénarié J (1980) Sequential analysis of the organogenesis of lucerne (*Medicago sativa*) root nodules using symbiotically-defective mutants of *Rhizobium meliloti*. Differentiation **16:** 163–172

Utrup LJ, Cary AJ, Hanks Norris JH (1993) Five nodulation mutants of white sweetclover (*Melilotus alba* Desr.) exhibit distinct phenotypes blocked at root hair curling, infection thread development, and nodule organogenesis. Plant Physiol **103:** 925–932

Vance CP, Johnson LEB (1983) Plant determined ineffective nodules in alfalfa (*Medicago sativa*): structural and biochemical comparisons. Can J Bot **61:** 93–106

Vasse J, de Billy F, Camut S, Truchet G (1990) Correlation between ultrastructural differentiation of bacteroids and nitrogen fixation in alfalfa nodules. J Bacteriol **172:** 4295–4306

Vasse J, de Billy F, Truchet G (1993) Abortion of infection during the *Rhizobium meliloti*-alfalfa symbiotic interaction is accompanied by a hypersensitive reaction. Plant J **4:** 555–566

Vincent JM (1980) Factors controlling the legume *Rhizobium* symbiosis. *In* WE Newton, WH Orme-Johnson, eds, Nitrogen Fixation, Vol II. University Park Press, Baltimore, MD, pp 103–129

Weeden NF, Kneen BE, Larue TA (1990) Genetic analysis of *sym* genes and other nodule related genes in *Pisum sativum*. *In* P Gresshoff, LE Roth, G Stacey, WE Newton, eds, Nitrogen Fixation: Achievements and Objectives. Chapman and Hall, New York, pp 323–329

Yang C, Signer ER, Hirsch AM (1992) Nodules initiated by *Rhizobium meliloti* exopolysaccharide mutants lack a discrete, persistent nodule meristem. Plant Physiol **98:** 143–151